

## Nutrient modulation of polarized and sustained submembrane $\text{Ca}^{2+}$ microgradients in mouse pancreatic islet cells

Ivan Quesada\*†, Franz Martín†‡ and Bernat Soria\*†

\*Department of Physiology, †Institute of Bioengineering and ‡Department of Genetics, Nutrition and Toxicology, Campus de San Juan, Aptdo. 18, University Miguel Hernandez, 03550 San Juan, Alicante, Spain

(Received 4 January 2000; accepted 1 March 2000)

1. The intracellular calcium concentration ( $[\text{Ca}^{2+}]_i$ ) near the plasma membrane was measured in mouse pancreatic islet cells using confocal spot detection methods.
2. Whereas small cytosolic  $\text{Ca}^{2+}$  gradients were observed with 3 mM glucose, a steeper sustained gradient restricted to domains beneath the plasma membrane (space constant,  $0.67 \mu\text{m}$ ) appeared with 16.7 mM glucose.
3. When the membrane potential was clamped with increasing  $\text{K}^+$  concentrations (5, 20 and 40 mM), no  $[\text{Ca}^{2+}]_i$  gradients were observed in any case.
4. Increasing glucose concentration (0, 5 and 16.7 mM) in the presence of  $100 \mu\text{M}$  diazoxide, a  $\text{K}^+$  channel opener, plus 40 mM  $\text{K}^+$  induced steeper  $[\text{Ca}^{2+}]_i$  gradients, confirming the role of membrane potential-independent effects of glucose.
5. Prevention of  $\text{Ca}^{2+}$  store refilling with  $30 \mu\text{M}$  cyclopiazonic acid (CPA) or blockade of uniporter-mediated  $\text{Ca}^{2+}$  influx into the mitochondria with  $1 \mu\text{M}$  carbonyl cyanide *m*-chlorophenyl hydrazone (CCCP) or  $1 \mu\text{M}$  Ru-360 significantly reduced the steepness of the 16.7 mM glucose-induced  $[\text{Ca}^{2+}]_i$  gradients.
6. Measured values of  $[\text{Ca}^{2+}]_i$  reached  $6.74 \pm 0.67 \mu\text{M}$  at a distance of  $0.5 \mu\text{m}$  from the plasma membrane and decayed to  $0.27 \pm 0.03 \mu\text{M}$  at a distance of  $2 \mu\text{m}$ . Mathematically processed values at 0.25 and  $0 \mu\text{m}$  gave a higher  $[\text{Ca}^{2+}]_i$ , reaching  $8.18 \pm 0.86$  and  $10.05 \pm 0.98 \mu\text{M}$ , respectively.
7. The results presented indicate that glucose metabolism generates  $[\text{Ca}^{2+}]_i$  microgradients, which reach values of around  $10 \mu\text{M}$ , and whose regulation requires the involvement of both mitochondrial  $\text{Ca}^{2+}$  uptake and endoplasmic reticulum  $\text{Ca}^{2+}$  stores.

Many mechanisms of exocytosis in excitable secretory cells are located at the cell membrane and are regulated by the  $[\text{Ca}^{2+}]_i$  just beneath the plasma membrane. The observation that exocytosis is triggered more effectively by agents that stimulate  $\text{Ca}^{2+}$  influx than by those that mobilize intracellular  $\text{Ca}^{2+}$  led to the suggestion that spatially localized  $[\text{Ca}^{2+}]$  increases might be responsible for triggering exocytosis (Augustine & Neher, 1992). Models of  $\text{Ca}^{2+}$  entry, binding and diffusion (Sala & Hernandez-Cruz, 1990) have predicted that the opening of  $\text{Ca}^{2+}$  channels causes the formation of  $\text{Ca}^{2+}$  gradients ( $\text{Ca}^{2+}$  microdomains) reaching a concentration of tens or hundreds of micromolar just beneath the plasma membrane. This has been confirmed by digital imaging using a 'no neighbours' deblurring filter in chromaffin cells (Monck *et al.* 1994). As supported by several pieces of evidence, in order to generate these  $\text{Ca}^{2+}$  microdomains without a high energy cost, the  $\text{Ca}^{2+}$  homeostasis within cells needs to be highly co-ordinated and strongly

related to the cellular energetic economy (Petersen *et al.* 1994; Berridge, 1998).

In pancreatic  $\beta$ -cells the main physiological secretagogues are metabolized by the cell, causing an increase in the ATP/ADP ratio and the diadenosine polyphosphate concentration (Ripoll *et al.* 1996; Martín *et al.* 1998), which leads to the closure of ATP-sensitive  $\text{K}^+$  ( $\text{K}_{\text{ATP}}$ ) channels and depolarization of the plasma membrane potential (Ashcroft & Rorsman, 1989). This in turn leads to  $\text{Ca}^{2+}$  influx through voltage-gated  $\text{Ca}^{2+}$  channels and a rise in cytosolic  $[\text{Ca}^{2+}]$  (Dunne & Petersen, 1991; Wollheim *et al.* 1996). Recent studies using a combination of techniques have demonstrated that, as predicted by the models, the insulin-containing secretory granules and the voltage-dependent  $\text{Ca}^{2+}$  channels co-localize within the  $\beta$ -cell (Bokvist *et al.* 1995). In addition, stimulatory glucose concentrations induced steep spatial gradients of  $[\text{Ca}^{2+}]_i$  in the vicinity of

the plasma membrane (Martín *et al.* 1997). The complex interplay between  $\text{Ca}^{2+}$  influx and the  $\text{Ca}^{2+}$  release and uptake mechanisms activated by nutrient secretagogues suggests that physiological stimulators may influence the  $\text{Ca}^{2+}$  microdomains through additional regulatory systems.

Although radial gradients in  $[\text{Ca}^{2+}]_i$  have been estimated in pancreatic  $\beta$ -cells using digital imaging techniques (Theiler *et al.* 1992; Bokvist *et al.* 1995; Martín *et al.* 1997), a direct measurement of submembrane  $[\text{Ca}^{2+}]_i$  is still lacking. In addition, these gradients are much smaller in magnitude than predicted for secretory cells (Klingauf & Neher, 1997). This suggests that although large  $[\text{Ca}^{2+}]_i$  changes immediately beneath the cell membrane do occur, they are in many cases obscured. This may be attributed, at least in part, to limitations in currently available imaging technology.

One strategy for selectively monitoring near-membrane  $[\text{Ca}^{2+}]$  changes is to use a probe that only indicates  $[\text{Ca}^{2+}]$  directly beneath the membrane by virtue of its localized distribution (Etter *et al.* 1994; Blatter & Niggli, 1998). Alternatively, confocal spot detection methods (Escobar *et al.* 1994; Quesada *et al.* 1998) would also be a powerful tool for selectively monitoring the near-membrane  $[\text{Ca}^{2+}]$ . In this study, the successful use of a PIN photodiode connected to a high-gain patch-clamp amplifier, together with the optical configuration of the system made the detection of sustained submembrane  $\text{Ca}^{2+}$  gradients in pancreatic islet cells possible, with an excellent signal-to-noise ratio. Moreover, we were able to use this new method to measure and characterize the glucose-induced  $[\text{Ca}^{2+}]_i$  gradients within the first  $2\ \mu\text{m}$  of the plasma membrane. Finally, we provide evidence indicating that glucose regulates the  $[\text{Ca}^{2+}]_i$  gradients through mitochondrial  $\text{Ca}^{2+}$  uptake and the involvement of endoplasmic reticulum (ER)  $\text{Ca}^{2+}$  stores.

## METHODS

### Islet cell isolation and perfusion

Islets from adult (8–10 weeks old) Swiss albino male mice (OF1), killed by cervical dislocation in accordance with national guidelines, were isolated as previously described (Lenmark, 1974). Briefly, after pancreas digestion with collagenase (collagenase A, Boehringer Mannheim, Mannheim, Germany) in a stationary bath at  $37\ ^\circ\text{C}$ , islets were separated by centrifugation and hand picked under a stereomicroscope. Once isolated, islets were dispersed into single cells by enzymatic digestion in the presence of 0.05% trypsin plus 0.02% EDTA for 3 min. Cells were plated onto coverslips and cultured overnight in RPMI 1640 supplemented with 10% fetal calf serum, 100 i.u.  $\text{ml}^{-1}$  penicillin, 0.1  $\text{mg}\ \text{ml}^{-1}$  streptomycin and 5.6  $\text{mM}$  glucose (Martín *et al.* 1997).

### Loading and perfusion of islet cells

Islet cells were loaded with  $2\ \mu\text{M}$  fluo-3 AM (Molecular Probes) by a 60 min incubation at room temperature in the above-mentioned culture medium. Laser-scanning confocal microscopy (Leica TCS-NT System, Germany) was used to confirm the homogeneous distribution of the dye in the cytoplasm of the islet cells. The confocal detector aperture was set at  $64.3\ \mu\text{m}$  and a  $\times 40$  Pl Fluotar Leica objective was used. After acquiring eight optical slices of  $100\ \mu\text{m} \times 100\ \mu\text{m} \times 1\ \mu\text{m}$ , a uniform localization of fluo-3

throughout the cytoplasm of the pancreatic islet cells (in the presence of 3  $\text{mM}$  glucose) was observed (80%; Fig. 2A,  $n = 5$ ). The same uniform localization of fluo-3 throughout the cytoplasm was observed in the presence of 16.7  $\text{mM}$  glucose (data not shown;  $n = 4$ ).

For all cases, pancreatic islet cells were perfused at a rate of  $0.5\ \text{ml}\ \text{min}^{-1}$  with a modified Krebs-Ringer buffer (mM): 119 NaCl, 4.7 KCl, 1.2  $\text{MgSO}_4$ , 1.2  $\text{KH}_2\text{PO}_4$ , 25  $\text{NaHCO}_3$  and 2.5  $\text{CaCl}_2$ , constantly bubbled with a mixture of 95%  $\text{O}_2$ , 5%  $\text{CO}_2$ , giving a final pH of 7.4, plus the different agents applied in each experiment. Diazoxide, CPA and CCCP were obtained from Sigma; Ru-360 was from Calbiochem-Novabiochem GmbH (Bad Soden, Germany). All experiments were performed at  $37\ ^\circ\text{C}$ .

### Confocal spot detection of submembrane $\text{Ca}^{2+}$ microgradients

Cells were placed in a specimen chamber mounted on the stage of an inverted epifluorescence microscope (Nikon-Diaphot, Nikon, Tokyo, Japan) modified for confocal spot detection (Fig. 1A). The cell images were acquired with a cooled CCD camera (MCD-220, Spectra Source, Agoura Hills, CA, USA) using an oil-immersion  $\times 100$  Plan Fluor phase objective lens (numerical aperture (NA), 1.3; Nikon). The bright-field images shared the optics pathway with the confocal illumination, so the position of the spot could be followed throughout the experiments. The spot illumination–detection configuration was similar to that described previously (Escobar *et al.* 1994; Quesada *et al.* 1998). The illumination source was a multiline argon laser (5 W, Innova-70, Coherent Inc., Santa Clara, CA, USA). A spatial Gaussian filter allowed reduction of the laser beam diameter ( $\varnothing = 50\ \mu\text{m}$ ) and selection of the Gaussian profile of illumination (Fig. 1B). The resulting beam illuminated a  $10\ \mu\text{m}$  pinhole and was then focused into a spot on a cell through the  $\times 100$  objective lens (arrow in Fig. 2B). The full-width half-maximal (FWHM) dimension of the illumination spot was  $0.6\ \mu\text{m}$ , measured with the CCD camera in the same experimental conditions and analysed with the image analysis software. Changes in fluorescence were recorded by aligning and focusing the illumination spot onto the photosensitive area ( $\varnothing = 100\ \mu\text{m}$ ) of a photodiode (HR008, UDT, Hawthorne, CA, USA) mounted on a three-axis positioner (Newport, Irvine, CA, USA) with a detected dark current of less than 100 pA. The predicted detection volume was approximately  $0.6 \times 0.6 \times 1.1\ \mu\text{m}^3$ . The current output of the photodiode was amplified using an Axopatch 200A amplifier (50  $\text{G}\Omega$  feedback; Axon Instruments). The output voltages were filtered with an eight-pole Bessel filter (Frequency Devices, Haverhill, MA, USA) at corner frequencies of 2 kHz. Shutters (Uniblitz, Vincent Associates, Rochester, NY, USA) placed in the laser pathway controlled the illumination time (30 ms). The  $x$ – $y$ -axis position of the spot was controlled by stepper motorized translation stages (Newport), whilst a piezoelectric device controlled the fine  $z$ -axis movement of the objective. The fluorescence signals were always recorded from the equatorial plane of each cell. The signal-to-noise ratio of the system was 20 pA/0.18 pA. A home-made program installed in a Pentium computer controlled data acquisition, movement of stepper motors and illumination exposure time.

$\text{Ca}^{2+}$ -dependent fluo-3 fluorescence ( $F$ ) was expressed as  $F/F_{\text{max}}$  in order to normalize data.  $F_{\text{max}}$  (maximal fluorescence) was recorded after each experiment in the modified Krebs-Ringer buffer under conditions of saturating  $[\text{Ca}^{2+}]_i$  and in the absence of  $\text{Na}^{2+}$  (mM: 85 LiCl, 40 KCl, 1.2  $\text{MgSO}_4$ , 1.2  $\text{KH}_2\text{PO}_4$ , 25  $\text{NaHCO}_3$  and 10  $\text{CaCl}_2$ , with 10  $\mu\text{M}$  ionomycin). Since fluorescence values were below  $F_{\text{max}}$ , conditions were not saturating for the dye.  $F_{\text{min}}$  (minimum fluorescence) was calculated by lysing the cells with 50  $\mu\text{M}$  digitonin (Sigma) to obtain the background fluorescence

( $F_{\text{bkg}}$ ). From  $F_{\text{max}}$  and  $F_{\text{bkg}}$ , the value of  $F_{\text{min}}$  can be calculated as proposed by Nadal *et al.* (1996). The data were fitted to the standard calibration equation of Grynkiewicz *et al.* (1985) and used to calculate  $[Ca^{2+}]_i$ :

$$[Ca^{2+}]_i = K_d (F - F_{\text{min}}) / (F_{\text{max}} - F).$$

The  $K_d$  value of the fluo-3 batch, measured as previously described (Escobar *et al.* 1997), was  $0.69 \pm 0.02 \mu\text{M}$ .

Autofluorescence was  $< 3\%$ . Photobleaching was only 5% after ten consecutive 30 ms illumination pulses at the same point of detection ( $n = 6$ ).

### Experimental procedure

In order to explore the submembrane  $[Ca^{2+}]$  gradients, the cell equatorial plane was selected, followed by the positioning of eight detection spots around the cell but immediately beneath the plasma membrane with a separation distance of  $1 \mu\text{m}$  in the presence of the different stimuli (glucose or  $K^+$ ). Then, the area of highest fluorescence delimited by one of the eight spots was selected (Fig. 2C). Finally, cells were perfused for 5 min (or 2 min for KCl experiments; steady-state conditions) with the modified Krebs-Ringer buffer plus the different agents, and the first  $2 \mu\text{m}$  beneath the plasma membrane were explored during the last 30 s of the stimulus at seven detection spots ( $0.5, 0.65, 0.8, 1.0, 1.25, 1.5$  and  $2.0 \mu\text{m}$ ) at 5 s intervals for each distance, as shown schematically in Fig. 2D. The small overlapping distance between each two adjacent spots did not interfere with the results obtained as photobleaching was minimized. For plots of the data, each point is the value of the spot fluorescence ( $\emptyset = 0.6 \mu\text{m}$ ) and its position was calculated as the distance between the plasma membrane and the centre of the spot. To randomize the measurements, the procedure was also inverted and spot detection experiments were performed starting

with the point furthest from the plasma membrane ( $2 \mu\text{m}$ ) in the presence of  $16.7 \text{ mM}$  glucose. Data are expressed as means  $\pm$  s.e.m.

### Mathematical estimation of $[Ca^{2+}]_i$ close to the plasma membrane

Due to the fact that the limit of the edge of the closest spot ( $0.5 \mu\text{m}$ ) was only  $0.2 \mu\text{m}$  away from the plasma membrane, closer points to the membrane were unreliable because a part of the spot detection area was out of the cell in the  $z$ -axis as a consequence of cell curvature. To obtain the  $[Ca^{2+}]_i$  at distances smaller than  $0.5 \mu\text{m}$  from the plasma membrane a mathematical approach was used. Since geometric characteristics of the illumination spot and the equatorial plane of the cell are known, the fluorescence detection volume for each distance, which results from the interaction between the cell and the illumination spot, can be calculated using the following function:

$$F(x) = (2 - 3x + x^3) / 4,$$

where  $x$  is  $d/a$ ,  $d$  is the distance from the centre of the illumination spot to the plasma membrane and  $a$  is the radius of the illumination spot. Thus, estimated fluorescence values for these distances ( $0$  and  $0.25 \mu\text{m}$ ) can be generated with the mathematical approach from the measured fluorescence values of partially out of cell spots whose distance from the plasma membrane can be finely controlled.

## RESULTS

### Polarity of the $Ca^{2+}$ signal

In order to avoid the effect of a minimization of the fluorescence signal due to ion diffusion over the distance from the point of  $Ca^{2+}$  entry to the area of recording,  $Ca^{2+}$

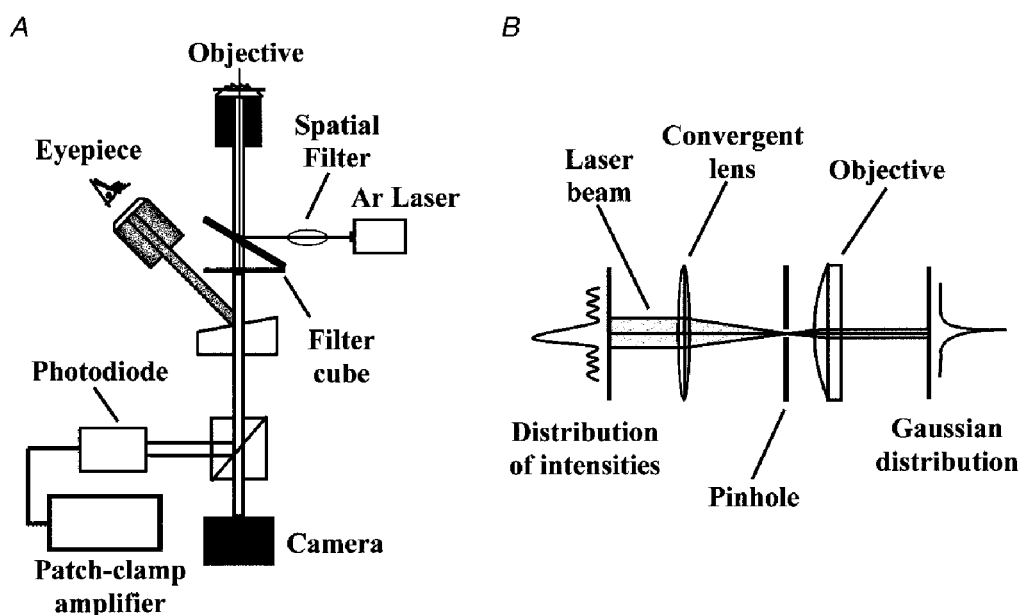


Figure 1. Schematic diagram of the experimental set-up

A, basic optical components: an inverted microscope equipped with a standard epifluorescence port, a Peltier cooled CCD camera used to image the cells and the position of the spot, a beam splitter to split bright-field images from emitted fluorescence light, an argon laser which provides the high-intensity monochromatic light used to excite the fluorescence dyes, a spatial filter, a photodiode centred on the spot to record the fluorescence emitted by the cells, and a high-gain patch-clamp amplifier to convert the fluorescence intensity to current. B, schematic design of the Gaussian spatial filter which in combination with the objective focuses the beam into a spot on the preparation.

gradients were only studied in areas with a noticeable localization of the  $\text{Ca}^{2+}$  signal and with the highest fluorescence values. Thus, eight equidistant detection spots were positioned around the cell but immediately beneath the plasma membrane (Fig. 2C) with a separation distance of  $1\ \mu\text{m}$  in the presence of the different stimuli (16.7 mM glucose, 3 mM glucose or 40 mM extracellular  $\text{K}^+$  ( $\text{K}_o^+$ )). Polarity was assumed when significant differences (higher than 30%) in fluorescence values from one position with respect to other positions appeared (Fig. 2C); 86 and 76% of the cells were polarized with 16.7 mM glucose ( $n = 29$ ) and 40 mM  $\text{K}^+$  ( $n = 21$ ), respectively. In addition, polarized cells (81%) were also observed with 3 mM glucose ( $n = 21$ ). Thus, a remarkable spatial distribution of  $\text{Ca}^{2+}$  appeared in the majority of cells. Since the equatorial plane was selected to detect  $\text{Ca}^{2+}$  gradients, it was possible that some of these gradients could be attenuated because of  $\text{Ca}^{2+}$  diffusion to other areas. Thus, to minimize this diffusion process, gradients were only studied in cells showing the highest polarity of the signal and in areas of maximal polarity.

### Detection of submembrane $\text{Ca}^{2+}$ gradients modulated by glucose

To study the  $\text{Ca}^{2+}$  gradients, the first  $2\ \mu\text{m}$  beneath the plasma membrane were explored using several detection spots (0.5, 0.65, 0.8, 1.0, 1.25, 1.5 and  $2.0\ \mu\text{m}$ ) at 5 s intervals for each distance, as shown schematically in Fig. 2D. As shown in Fig. 3, pancreatic islet cells stimulated with different nutrient and non-nutrient agents showed submembrane  $\text{Ca}^{2+}$  gradients with different characteristics. Note that in all cases, the gradients were localized to restricted domains beneath the plasma membrane.

Figure 3A shows the effect of different glucose concentrations on the  $\text{Ca}^{2+}$  gradients ( $n = 7$ ). Cells stimulated with 16.7 mM glucose showed a steeper  $\text{Ca}^{2+}$  gradient than when stimulated with 3 mM glucose. The same  $\text{Ca}^{2+}$  gradient ( $n = 4$ ) was observed when starting the measurements at the point furthest from the plasma membrane (data not shown). Since this submembrane  $\text{Ca}^{2+}$  distribution was glucose induced, such  $\text{Ca}^{2+}$  gradients should be due to the interplay

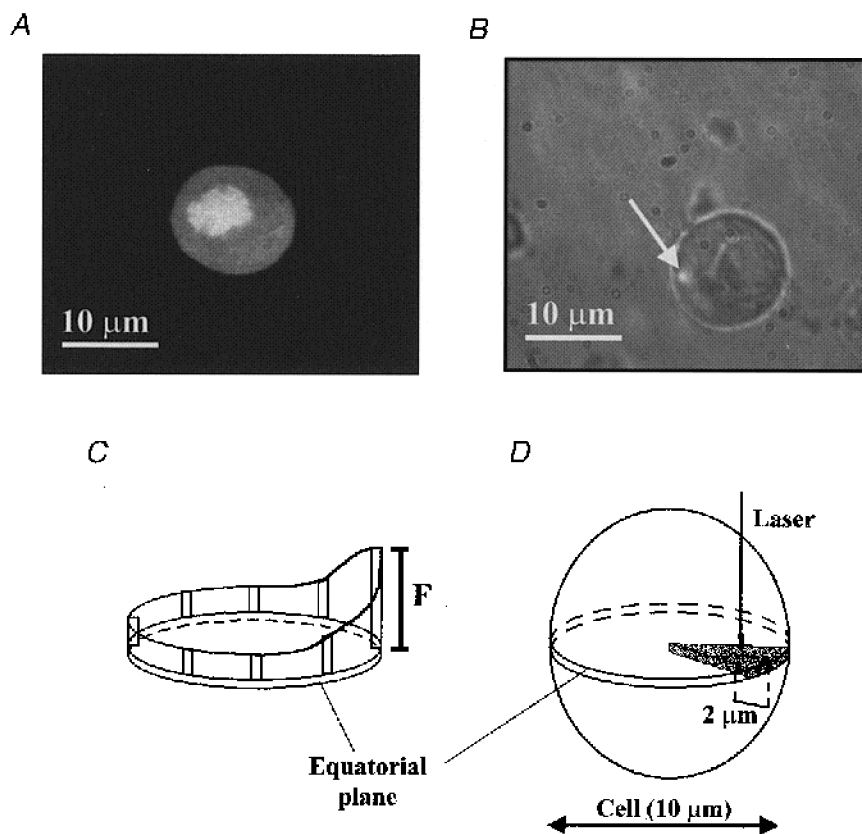


**Figure 2.** Confocal spot detection of submembrane  $\text{Ca}^{2+}$  microgradients

A, confocal fluorescence image of a fluo-3-loaded pancreatic islet cell, in the presence of 3 mM glucose, showing the distribution of the fluo-3 fluorescence. B, phase-contrast image ( $\times 100$  lens) of a cultured pancreatic islet cell ( $\text{O} = 10\ \mu\text{m}$ ) with the fluorescence illumination spot (arrow;  $0.6 \times 0.6 \times 1.1\ \mu\text{m}^3$  fluorescence detection volume) focused near to the plasma membrane. C and D, schematic design of the experimental procedure: (i) selection of the cell equatorial plane; (ii) localization of the area of polarity; and (iii) perfusion of the cells for 5 min with Krebs-Ringer buffer plus the different agents. In the last 30 s of the stimulus the first  $2\ \mu\text{m}$  beneath the plasma membrane were explored using seven detection spots (0.5, 0.65, 0.8, 1.0, 1.25, 1.5 and  $2.0\ \mu\text{m}$ ) at 5 s intervals for each distance.

between the extracellular  $\text{Ca}^{2+}$  source and the internal  $\text{Ca}^{2+}$  sinks. The higher  $[\text{Ca}^{2+}]_i$  reached close to the plasma membrane in the presence of 16.7 mM glucose (compared with 3 mM glucose) is due to a higher  $\text{Ca}^{2+}$  influx through voltage-dependent  $\text{Ca}^{2+}$  channels, as has previously been described (Ashcroft & Rorsman, 1989). The  $\text{Ca}^{2+}$  activity profile at distinct glucose concentrations suggests a role for glucose in creating these steep gradients as much in the extracellular  $\text{Ca}^{2+}$  source as in the internal  $\text{Ca}^{2+}$  sinks, since when removed, the submembrane  $\text{Ca}^{2+}$  gradient disappeared and a homogeneous spatial  $\text{Ca}^{2+}$  distribution was observed throughout the cytosol. Furthermore, in the absence of glucose, a higher  $[\text{Ca}^{2+}]_i$  was observed in the plateau, when compared with that in the presence of glucose.

When the membrane potential was clamped with increasing  $\text{K}^+$  concentrations (5, 20 and 40 mM) in the presence of 3 mM glucose (Fig. 3B), subsequent voltage-dependent effects on  $\text{Ca}^{2+}$  patterns were observed. As shown in Fig. 3B,  $\text{K}^+$  induced an increase in the  $[\text{Ca}^{2+}]_i$ , whilst maintaining the same  $\text{Ca}^{2+}$  pattern as observed with 3 mM glucose (Fig. 3A). In all cases,  $\text{Ca}^{2+}$  gradients had the same spatial distribution but different amplitudes ( $n = 7$ ), but no significant gradient was detected in any case.

In order to distinguish between membrane potential-dependent and -independent effects of glucose in this phenomenon (Fig. 3C), membrane potential was clamped by exposing the pancreatic islet cells ( $n = 7$ ) to 100  $\mu\text{M}$  diazoxide to avoid the effects of glucose on membrane potential and 40 mM  $\text{K}^+$  to depolarize the membrane, then different glucose concentrations (0, 5 and 16.7 mM) were applied (Nadal *et al.* 1994; Miura *et al.* 1997). Under these conditions, by increasing the glucose concentration it was possible to induce steeper  $\text{Ca}^{2+}$  gradients, showing an involvement of glucose in the internal buffering of the  $\text{Ca}^{2+}$  influx induced by 40 mM  $\text{K}^+$ . Conversely, lowering the glucose concentration (5 mM) attenuated this effect on the  $\text{Ca}^{2+}$  gradient (Fig. 3C). Finally, no submembrane  $\text{Ca}^{2+}$  gradient was observed in the absence of glucose.

#### Sustained response to the stimulation

In order to find out the temporal pattern of these submembrane  $\text{Ca}^{2+}$  gradients, the following protocol was designed. A detection spot was positioned at 1  $\mu\text{m}$  under the plasma membrane in the area of maximal polarization of the signal (see Methods) and cells were perfused with 16.7 mM glucose ( $n = 6$ ). After 5 min stimulation, cells were illuminated at the same spatial point with four consecutive laser pulses (30 ms) with a time separation of 5 s. After 30 s the cell received the same sequence of pulses. This protocol was repeated after 10 min. Other distances from the plasma membrane were also tested (0.5, 1.5 and 2  $\mu\text{m}$ ). In all cases the results indicated that once established there was no time-dependent variation of the  $\text{Ca}^{2+}$ -dependent fluorescence signal for each spot of detection, so sustained  $\text{Ca}^{2+}$  gradients could be assumed during stimulation. The same protocol

was performed with 3 mM glucose and 40 mM  $\text{K}^+$  and similar results were observed ( $n = 5$ ).

#### Effects of SERCA pump inhibition on submembrane $\text{Ca}^{2+}$ gradients

CPA, the specific inhibitor of the sarcoplasmic reticulum (SR)-ER  $\text{Ca}^{2+}$ -ATPase (SERCA) pump family (Demaurex *et al.* 1992), has been used to show the role of intracellular  $\text{Ca}^{2+}$

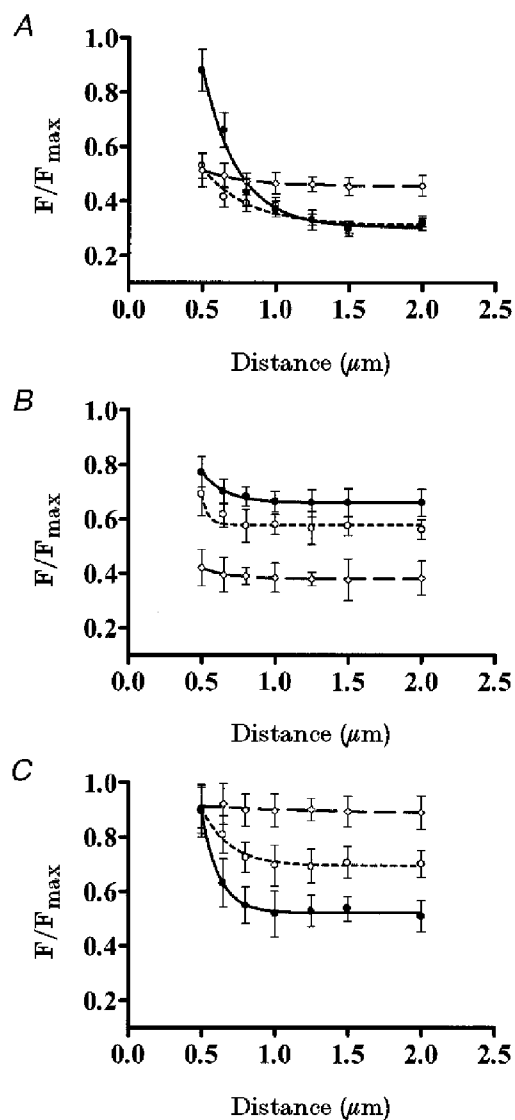


**Figure 3.** Submembrane  $\text{Ca}^{2+}$  gradients modulated by physiological stimuli

A, pancreatic islet cells were perfused with different glucose concentrations: 16.7 mM (●, continuous line), 3 mM (○, short-dash line) and 0 mM (◇, long-dash line) ( $n = 7$  cells). B, pancreatic islet cells were perfused in the presence of 3 mM glucose with different  $\text{K}^+$  concentrations: 40 mM (●, continuous line), 20 mM (○, short-dash line) and 5 mM (◇, long-dash line) ( $n = 7$  cells). C, pancreatic islet cells were perfused with different glucose concentrations: 16.7 mM (●, continuous line), 5 mM (○, short-dash line) and 0 mM (◇, long-dash line), in the presence of 40 mM  $[\text{K}^+]_o$  and 100  $\mu\text{M}$  diazoxide ( $n = 7$  cells).

stores in  $\text{Ca}^{2+}$  signalling (Nadal *et al.* 1996). Since the previous  $\text{Ca}^{2+}$  output from intracellular stores through leak channels could mask the submembrane  $\text{Ca}^{2+}$  gradients, recordings started after 5 min of perfusing cells with CPA. Figure 4A shows the effect of 30  $\mu\text{M}$  CPA on the 16.7 mM glucose-induced  $\text{Ca}^{2+}$  gradient ( $n = 6$ ). CPA caused a significant reduction in the steepness of the  $\text{Ca}^{2+}$  gradient by abolishing a cytoplasmic element of the  $\text{Ca}^{2+}$  sink system. This experiment proves the involvement of the ATP-dependent SERCA pumps in the origin of the submembrane  $\text{Ca}^{2+}$  gradients.

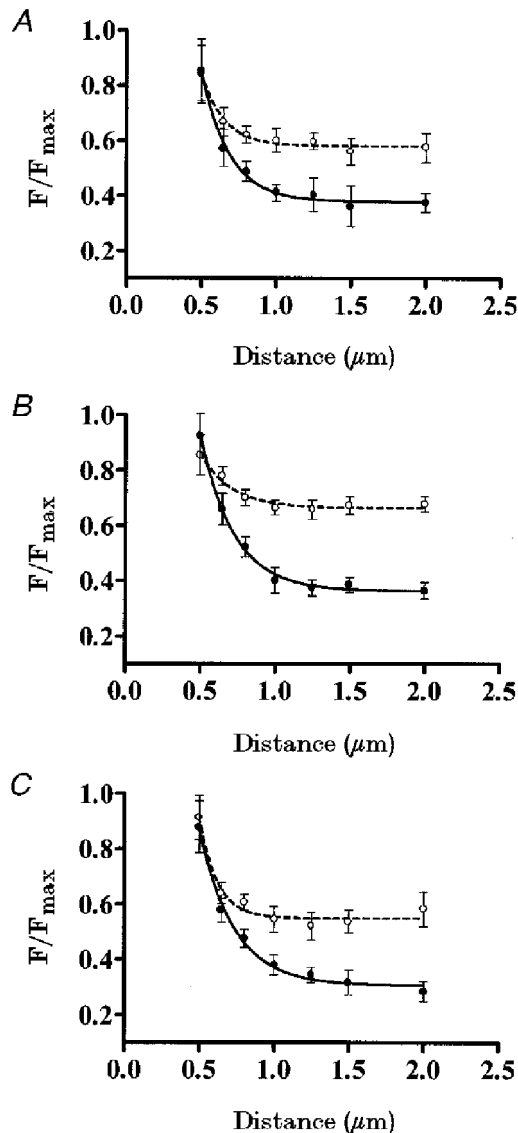


**Figure 4.** Homeostatic mechanisms involved in  $\text{Ca}^{2+}$  gradients

A, pancreatic islet cells were perfused with 16.7 mM glucose (●) and with 16.7 mM glucose plus 30  $\mu\text{M}$  CPA (○) ( $n = 6$  cells). B, pancreatic islet cells were perfused with 16.7 mM glucose (●) and with 16.7 mM glucose plus 1  $\mu\text{M}$  CCCP (○) ( $n = 5$  cells). C, pancreatic islet cells were perfused with 16.7 mM glucose (●) and with 16.7 mM glucose plus 1  $\mu\text{M}$  Ru-360 (○) ( $n = 6$  cells).

### Role of mitochondria in submembrane $\text{Ca}^{2+}$ gradients

Since clearance of cytosolic  $\text{Ca}^{2+}$  by mitochondria can be perturbed when the mitochondrial membrane potential ( $\Psi_m$ ) is altered or the  $\text{Ca}^{2+}$  uniporter is blocked (Maechler *et al.* 1997), CCCP protonophore and the specific inhibitor of mitochondrial  $\text{Ca}^{2+}$  uptake Ru-360 (Matlib *et al.* 1998) were used for this purpose in order to ascertain the involvement of this organelle in the generation of the  $\text{Ca}^{2+}$  gradients. In these experiments the participation of the mitochondrial stores in the  $\text{Ca}^{2+}$  gradients was tested in the presence of 16.7 mM glucose ( $n = 6$ ). For experiments involving 1  $\mu\text{M}$  CCCP, recordings started after 5 min of perfusing the cells. Figure 4B shows that when  $\Delta\Psi_m$  was diminished with 1  $\mu\text{M}$  CCCP, the 16.7 mM glucose-induced  $\text{Ca}^{2+}$  gradient was smaller, indicating a putative role for the mitochondrial store as a  $\text{Ca}^{2+}$  sink. The same effect was observed when the isolated pancreatic islet cells (Fig. 4C;  $n = 6$ ) were perfused for 5 min with 1  $\mu\text{M}$  Ru-360.

### $[\text{Ca}^{2+}]_i$ close to the plasma membrane

We were interested in estimating the  $[\text{Ca}^{2+}]_i$  in the first 0.5  $\mu\text{m}$  beneath the plasma membrane in order to find out the  $[\text{Ca}^{2+}]_i$  directly 'seen' by secretory granules during glucose stimulation near a channel pore. Due to the fact that reliable direct measurements were beyond our capabilities at these distances (see Methods), a mathematical approach was used. Figure 5 shows the measured values obtained with fluo-3 when cells were perfused with 16.7 mM glucose (●;  $n = 7$ ) and the calculated values for the two distances of 0 and 0.25  $\mu\text{m}$  (○). Measured values of  $[\text{Ca}^{2+}]_i$  reached  $6.74 \pm 0.67 \mu\text{M}$  at a distance of 0.5  $\mu\text{m}$  and decayed to  $0.27 \pm 0.03 \mu\text{M}$  at a distance of 2  $\mu\text{m}$ . Mathematically processed  $[\text{Ca}^{2+}]_i$  values obtained with signals from partially out of cell spots were higher, reaching  $8.18 \pm 0.86$  and  $10.05 \pm 0.98 \mu\text{M}$  at 0.25 and 0  $\mu\text{m}$ , respectively.

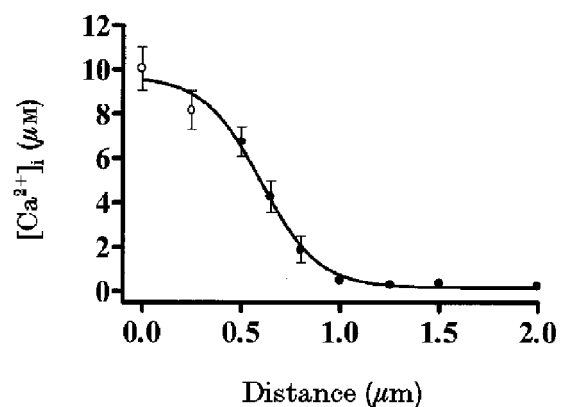


**Figure 5.**  $[\text{Ca}^{2+}]_i$  close to the plasma membrane

$[\text{Ca}^{2+}]_i$  in pancreatic islet cells loaded with fluo-3 and stimulated with 16.7 mM glucose (●) ( $n = 7$  cells). The experimental design is shown in Fig. 2D. The calibration equation of Grynkiewicz *et al.* (1985) was used to calculate  $[\text{Ca}^{2+}]_i$ , assuming a  $K_d$  of 0.69  $\mu\text{M}$  for fluo-3. A mathematical estimation of  $[\text{Ca}^{2+}]_i$  within a pancreatic islet cell at distances of 0 and 0.25  $\mu\text{m}$  beneath the plasma membrane is also shown (○).

## DISCUSSION

In this paper, we have described the use of a confocal spot technique in pancreatic islet cells (Fig. 1) to detect the existence of sustained polarized submembrane  $\text{Ca}^{2+}$  microgradients regulated by nutrient stimulators.

In secretory cells, mechanisms involved in the regulation of exocytosis and  $\text{Ca}^{2+}$  permeability are located at the cell membrane and are regulated by the  $[\text{Ca}^{2+}]_i$  just beneath the membrane. In pancreatic  $\beta$ -cells, recent studies (Bokvist *et al.* 1995; Martín *et al.* 1997) have demonstrated that the  $[\text{Ca}^{2+}]$  underneath the plasma membrane is very different from the  $[\text{Ca}^{2+}]$  in the bulk cytosol.

Nutrient secretagogues, through a membrane depolarization secondary to nutrient metabolism, raise  $\beta$ -cell  $[\text{Ca}^{2+}]_i$  and cause insulin release (Ashcroft & Rorsman, 1989). In contrast to fast synapses in which neurotransmitter release is mostly dependent on an extremely rapid  $[\text{Ca}^{2+}]$  increase ( $\leq 100 \mu\text{s}$ ), endocrine cells maintain hormone release for minutes to hours. Thus, regulation of exocytosis by localized (sustained  $\text{Ca}^{2+}$  microgradients) rather than global increases in  $[\text{Ca}^{2+}]_i$  is advantageous to the  $\beta$ -cell (Petersen *et al.* 1994) because the expenditure of metabolic energy to subsequently restore  $[\text{Ca}^{2+}]_i$  to the resting level is minimized. Given the importance of the increase of  $[\text{Ca}^{2+}]_i$  in restricted parts of the cell, it is not surprising to find a polarization of the  $\text{Ca}^{2+}$  microgradients in response to glucose. In this regard, polarity of the pancreatic islet cell even with non-stimulatory glucose concentrations confirms recent studies of Bokvist *et al.* (1995) that show that L-type  $\text{Ca}^{2+}$  channels of pancreatic  $\beta$ -cells are clustered in the regions containing the secretory granules, raising the interesting possibility that these regions could correspond to hot-spots of exocytosis. It now seems likely that  $\text{Ca}^{2+}$  homeostasis is very important for the presence of maintained  $\text{Ca}^{2+}$  microgradients and, as Nadal *et al.* (1994) suggested, the main mechanism responsible for  $\text{Ca}^{2+}$  homeostasis is dependent on metabolic energy directly provided by glucose metabolism. As a result, metabolism of glucose is a prerequisite for the maintenance of the steep spatial  $\text{Ca}^{2+}$  microgradients (Fig. 3A). The need for glucose to supply the energy demanded by this process was supported by the observation that in the absence of glucose (Fig. 3A) no submembrane  $\text{Ca}^{2+}$  microgradients were induced, whereas a small  $\text{Ca}^{2+}$  gradient was obtained with non-stimulatory glucose concentrations (Fig. 3A), indicating the presence of some ATP-dependent  $\text{Ca}^{2+}$  homeostatic mechanism with a high affinity for  $\text{Ca}^{2+}$  that can be activated with low ATP concentrations. Further evidence of the need for glucose metabolism is that high  $\text{Ca}^{2+}$  influx elicited by  $[\text{K}^+]_o$ -dependent voltage depolarization did not modify the steepness of the small  $\text{Ca}^{2+}$  gradient elicited by non-stimulatory glucose concentrations (Fig. 3B), since the fuel component given by the low glucose concentrations was not enough to counteract the high  $[\text{K}^+]$ -induced  $\text{Ca}^{2+}$  influx. Finally, nutrient-induced  $\text{Ca}^{2+}$  microgradients reflect the activation of glucose-dependent sequestering mechanisms.

This was demonstrated by using diazoxide (Fig. 3C), which opens  $\text{K}_{\text{ATP}}$  channels and permits clamping of the membrane potential at stable levels determined by the concentration of extracellular  $\text{K}^+$  (Nadal *et al.* 1994; Miura *et al.* 1997).

The ER and its specialized subcompartments are believed to be an important dynamic  $\text{Ca}^{2+}$  storage compartment of the cell. In fact, the overall  $\text{Ca}^{2+}$  content of the ER from different cell types has been found to be in the range 0.5–5 mM (Meldolesi & Pozzan, 1998). The effects of the SERCA pump blocker CPA on the glucose-induced  $\text{Ca}^{2+}$  microgradient (Fig. 4A) revealed the involvement of this  $\text{Ca}^{2+}$  store in modulating these  $\text{Ca}^{2+}$  gradients. The mechanisms involved in the function of the ER as a sustained sink need further investigation. However, the cellular architecture in low and high  $[\text{Ca}^{2+}]$  subcompartments within the ER proposed by Montero *et al.* (1997), and the dynamic interplay between them, suggests that the ER is heterogeneous in terms of  $\text{Ca}^{2+}$  handling and can contribute to the generation of the  $\text{Ca}^{2+}$  microgradients observed in pancreatic islet cells. Finally,  $[\text{Ca}^{2+}]_i$  increases in regions further from the plasma membrane should cause an elevation of  $[\text{Ca}^{2+}]_i$  near the location of the exocytotic machinery complex (e.g. the first 200 nm). Thus, an explanation for the finding that while the fluorescence signal increased in the presence of CPA in regions further from the plasma membrane, this signal did not increase accordingly near the membrane, is that given its  $K_d$  of  $0.69 \pm 0.02 \mu\text{M}$ , fluo-3 near the membrane is in almost saturating conditions, thus further  $[\text{Ca}^{2+}]$  increases cannot be detected. Other dyes (such as Calcium Green-2) would be able to detect the increase in  $[\text{Ca}^{2+}]_i$  near the plasma membrane, but due to its higher  $K_d$  the submicromolar  $\text{Ca}^{2+}$  levels present in the gradients would be difficult to see. However, the possibility cannot be excluded that  $\text{Ca}^{2+}$  can move from specific regions to other sites via an operational  $\text{Ca}^{2+}$  tunnel without any change in  $[\text{Ca}^{2+}]_i$  (Mogami *et al.* 1997).

Apart from the production of ATP, the major contribution of mitochondria to cell physiology lies in their impact on  $\text{Ca}^{2+}$  signalling. In fact, signals from populations of cells expressing mitochondrially targeted aequorin showed that mitochondria sequester  $\text{Ca}^{2+}$  from microdomains of locally high  $[\text{Ca}^{2+}]_i$  (Rizzuto *et al.* 1992). Moreover, other studies have concluded that mitochondria buffer  $\text{Ca}^{2+}$  reversibly with a  $\text{Ca}^{2+}$ -binding ratio of  $\sim 4000$  (Babcock *et al.* 1997; Xu *et al.* 1997). In this regard, in primary rat islet cells (Maechler *et al.* 1997) and  $\beta$ -cell line INS-1 cells (Kennedy *et al.* 1996) increases of glucose concentration in the physiological range caused a graded rise in mitochondrial  $\text{Ca}^{2+}$  concentration ( $[\text{Ca}^{2+}]_m$ ). Thus, mitochondrial  $\text{Ca}^{2+}$  uptake has an important role in the quantitative and spatiotemporal characteristics of  $[\text{Ca}^{2+}]_i$ . A crucial point, which is especially important in pancreatic  $\beta$ -cells, is to differentiate between changes in  $[\text{Ca}^{2+}]_i$  signal due specifically to reduced mitochondrial  $\text{Ca}^{2+}$  uptake, and changes due to ATP depletion that may follow a loss of  $\Delta\Psi_m$ , since depletion of ATP will clearly alter the

ability of cells to take up, extrude or sequester a  $\text{Ca}^{2+}$  load quite independently of mitochondrial  $\text{Ca}^{2+}$  uptake. The latter was shown in the present study by the addition of the ionophore CCCP to reduce  $\Delta\Psi_m$  and inhibit ATP production. This also disturbs  $\text{Ca}^{2+}$  influx via  $\text{K}_{\text{ATP}}$  channels and smaller  $\text{Ca}^{2+}$  fluorescence values were detected at  $0.5\ \mu\text{m}$  from the plasma membrane (Fig. 4B). In addition, the loss of  $\Delta\Psi_m$  prevents  $\text{Ca}^{2+}$  uptake by the mitochondria, resulting in higher fluorescence values at greater distances from the plasma membrane (more than  $0.65\ \mu\text{m}$ ; Fig. 4B). Finally, blockade of the mitochondrial  $\text{Ca}^{2+}$  uniporter greatly inhibits the clearance of  $\text{Ca}^{2+}$  from the cytosol in a direct manner, thus reducing the steepness of the  $\text{Ca}^{2+}$  microgradient (Fig. 4C). Note that Ru-360 specifically blocks  $\text{Ca}^{2+}$  uptake into mitochondria without any effect on ER  $\text{Ca}^{2+}$  uptake or release, L-type  $\text{Ca}^{2+}$  channel current and cytosolic  $\text{Ca}^{2+}$  transients (Matlib *et al.* 1998). All these data confirm the prediction of Kennedy *et al.* (1996) that in pancreatic  $\beta$ -cells the mitochondria are, to a significant extent, close to plasma membrane  $\text{Ca}^{2+}$  channels, and thus are strategically situated to sense the microdomains of high  $[\text{Ca}^{2+}]_i$  in their proximity and to fuel the exocytotic process. Moreover, some studies point to a tight local coupling of the ER and mitochondria (Duchen, 1999). The functional consequences of this local juxtaposition are: (i) mitochondria take up  $\text{Ca}^{2+}$  as it enters the cell and therefore limit the spatial spread of the  $[\text{Ca}^{2+}]_i$  signal, acting as a spatial buffer and modulating  $[\text{Ca}^{2+}]_i$  signalling; (ii) the increase in  $[\text{Ca}^{2+}]_m$  leads to increased activity of the mitochondrial metabolism, thereby facilitating exocytosis of insulin from secretory granules.

A growing body of evidence suggests that high  $\text{Ca}^{2+}$  concentrations are needed at exocytotic sites. Indeed, half-maximal rates of exocytosis required about  $16\ \mu\text{M}$   $\text{Ca}^{2+}$  underneath the plasma membrane in rat pituitary gonadotrophs (Tse *et al.* 1997),  $30\ \mu\text{M}$  in rat melanotrophs (Thomas *et al.* 1993) and  $50\ \mu\text{M}$  in bovine chromaffin cells (Augustine & Neher, 1992). In addition Bokvist *et al.* (1995) estimated that  $[\text{Ca}^{2+}]_i$  may well approach  $7\ \mu\text{M}$  following a 50 ms depolarization pulse for mouse pancreatic islet cells. Using the confocal spot detection technique together with a mathematical approximation for distances closer than  $0.5\ \mu\text{m}$  from the plasma membrane, we have found that, in mouse pancreatic islet cells,  $[\text{Ca}^{2+}]_i$  at the release sites peaks at approximately  $10\ \mu\text{M}$  after glucose stimulation. These values are close to those predicted by Klingauf & Neher (1997) after trains of depolarizations in excitable cells.

Our findings demonstrated that in pancreatic islet cells nutrient secretagogues induce  $\text{Ca}^{2+}$  microgradients which dissipate within the first micrometre from the membrane, and where  $[\text{Ca}^{2+}]_i$  readily reaches around  $10\ \mu\text{M}$ . Moreover, these pancreatic islet cells have a specialized and compartmentalized  $\text{Ca}^{2+}$  homeostatic machinery, mainly controlled by the mitochondria, ER and their close proximity to the plasma membrane, and designed to regulate  $[\text{Ca}^{2+}]_i$  at the exocytotic zone.

- ASHCROFT, F. M. & RORSMAN, P. (1989). Electrophysiology of the pancreatic  $\beta$ -cell. *Progress in Biophysics and Molecular Biology* **54**, 87–143.
- AUGUSTINE, G. J. & NEHER, E. (1992). Calcium requirements for secretion in bovine chromaffin cells. *Journal of Physiology* **450**, 247–271.
- BABCOCK, D. F., HARRINGTON, J., GOODWIN, P. C., PARK, Y. B. & HILLE, B. (1997). Mitochondrial participation in the intracellular  $\text{Ca}^{2+}$  network. *Journal of Cell Biology* **136**, 833–844.
- BERRIDGE, M. J. (1998). Neuronal calcium signalling. *Neuron* **21**, 13–26.
- BLATTER, L. A. & NIGGLI, E. (1998). Confocal near-membrane detection of calcium in cardiac myocytes. *Cell Calcium* **23**, 269–279.
- BOKVIST, K., ELIASSON, L., ÄMMÄLÄ, C., RENSTRÖM, E. & RORSMAN, P. (1995). Co-localization of L-type  $\text{Ca}^{2+}$  channels and insulin-containing secretory granules and its significance for the initiation of exocytosis in mouse pancreatic  $\beta$ -cells. *EMBO Journal* **14**, 50–57.
- DEMAUREX, N., LEW, D. & KRAUSE, K. H. (1992). Cyclopiazonic acid depletes intracellular  $\text{Ca}^{2+}$  stores and activates an influx pathway for divalent cations in HL-60 cells. *Journal of Biological Chemistry* **267**, 2318–2324.
- DUCHEN, M. R. (1999). Contributions of mitochondria to animal physiology: from homeostatic sensor to calcium signalling and cell death. *Journal of Physiology* **516**, 1–17.
- DUNNE, M. J. & PETERSEN, O. H. (1991). Potassium selective ion channels in insulin-secreting cells: physiology, pharmacology and their role in stimulus-secretion coupling. *Biochimica et Biophysica Acta* **1071**, 67–82.
- ESCOBAR, A. L., MONCK, J. R., FERNANDEZ, J. M. & VERGARA, J. L. (1994). Localization of the site of  $\text{Ca}^{2+}$  release at the level of a single sarcomere in skeletal muscle fibres. *Nature* **367**, 739–741.
- ESCOBAR, A. L., VELEZ, P., KIM, A. M., CIFUENTES, F., FILL, M. & VERGARA, J. L. (1997). Kinetic properties of DM-nitrophen and calcium indicators: rapid transient response to flash photolysis. *Pflügers Archiv* **434**, 615–631.
- ETTER, E. F., KUHN, M. A. & FAY, F. S. (1994). Detection of changes in near-membrane  $\text{Ca}^{2+}$  concentration using a novel membrane-associated  $\text{Ca}^{2+}$  indicator. *Journal of Biological Chemistry* **269**, 10141–10149.
- GRYNKIEWICZ, G., POENIE, M. & TSIEN, R. Y. (1985). A new generation of  $\text{Ca}^{2+}$  indicators with greatly improved fluorescence properties. *Journal of Biological Chemistry* **260**, 3440–3450.
- KENNEDY, E. D., RIZZUTO, R., THELER, J., PRALONG, W., BASTIANUTTO, C., POZZAN, T. & WOLLHEIM, C. B. (1996). Glucose-stimulated insulin secretion correlates with changes in mitochondrial and cytosolic  $\text{Ca}^{2+}$  in aequorin-expressing INS-1 cells. *Journal of Clinical Investigation* **98**, 2524–2538.
- KLINGAUF, J. & NEHER, E. (1997). Modeling buffered  $\text{Ca}^{2+}$  diffusion near the membrane: implications for secretion in neuroendocrine cells. *Biophysical Journal* **72**, 674–690.
- LENMARK, A. (1974). The preparation of, and studies on, free cell suspensions from mouse pancreatic islets. *Diabetologia* **10**, 431–438.
- MAEHLER, P., KENNEDY, E. D., POZZAN, T. & WOLLHEIM, C. B. (1997). Mitochondrial activation directly triggers the exocytosis of insulin in permeabilized pancreatic  $\beta$ -cells. *EMBO Journal* **16**, 3833–3841.
- MARTÍN, F., PINTOR, J., ROVIRA, J. M., RIPOLL, C., MIRAS-PORTUGAL, M. T. & SORIA, B. (1998). Intracellular diadenosine polyphosphates: a novel second messenger in the stimulus-secretion coupling. *FASEB Journal* **12**, 1499–1506.

- MARTÍN, F., RIBAS, J. & SORIA, B. (1997). Cytosolic  $\text{Ca}^{2+}$  gradients in pancreatic islet-cells stimulated by glucose and carbachol. *Biochemical and Biophysical Research Communications* **235**, 465–468.
- MATLIB, M. A., ZHOU, Z., KNIGHT, S., AHMED, S., CHOI, K. M., KRAUSE-BAUER, J., PHILLIPS, R., ALTSCHULD, R., KATSUBE, Y., SPERELAKIS, N. & BERS, D. M. (1998). Oxygen-bridged dinuclear ruthenium amine complex specifically inhibits  $\text{Ca}^{2+}$  uptake into mitochondria in vitro and in situ in single cardiac myocytes. *Journal of Biological Chemistry* **17**, 10223–10231.
- MELDOLESI, J. & POZZAN, T. (1998). The endoplasmic reticulum  $\text{Ca}^{2+}$  store: a view from the lumen. *Trends in Biological Sciences* **23**, 10–14.
- MIURA, Y., HENQUIN, J. C. & GILON, P. (1997). Emptying of intracellular  $\text{Ca}^{2+}$  stores stimulates  $\text{Ca}^{2+}$  entry in mouse pancreatic  $\beta$ -cells by both direct and indirect mechanisms. *Journal of Physiology* **503**, 387–398.
- MOGAMI, H., NAKANO, K., ТЕПИКИН, А. V. & PETERSEN, O. H. (1997).  $\text{Ca}^{2+}$  flows via tunnels in polarized cells: recharging of apical  $\text{Ca}^{2+}$  stores by focal  $\text{Ca}^{2+}$  entry through basal membrane patch. *Cell* **88**, 49–55.
- MONCK, J. R., ROBINSON, I. M., ESCOBAR, A., VERGARA, J. L. & FERNANDEZ, J. M. (1994). Pulsed laser imaging of rapid  $\text{Ca}^{2+}$  gradients in excitable cells. *Biophysical Journal* **67**, 505–514.
- MONTERO, M., ALVAREZ, J., SCHEENEN, W. J. J., RIZZUTO, R., MELDOLESI, J. & POZZAN, T. (1997). Calcium homeostasis in the endoplasmic reticulum: coexistence of high and low  $[\text{Ca}^{2+}]$  subcompartments in intact HeLa cells. *Journal of Cell Biology* **139**, 601–611.
- NADAL, A., FUENTES, E. & McNAUGHTON, P. A. (1996). Albumin stimulates uptake of calcium into subcellular stores in rat cortical astrocytes. *Journal of Physiology* **492**, 737–750.
- NADAL, A., VALDEOLMILLOS, M. & SORIA, B. (1994). Metabolic regulation of intracellular calcium concentration in mouse pancreatic islets of Langerhans. *American Journal of Physiology* **E769**–774.
- PETERSEN, O. H., PETERSEN, C. C. H. & KASAI, H. (1994). Calcium and hormone action. *Annual Review of Physiology* **56**, 297–319.
- QUESADA, I., MARTIN, F. & SORIA, B. (1998). Detection of submembrane cytosolic  $\text{Ca}^{2+}$  gradients by the laser spot confocal technique in pancreatic islet cells stimulated by nutrient secretagogues. *Journal of Physiology* **509.P**, 105P.
- RIPOLL, C., MARTIN, F., ROVIRA, J. M., PINTOR, J., MIRAS-PORTUGAL, M. T. & SORIA, B. (1996). Diadenosine polyphosphates: a novel class of glucose-induced intracellular messengers in the pancreatic  $\beta$ -cell. *Diabetes* **45**, 1431–1434.
- RIZZUTO, R., SIMPSON, A. W. M., BRINI, M. & POZZAN, T. (1992). Rapid changes of mitochondrial  $\text{Ca}^{2+}$  by specifically targeted recombinant aequorin. *Nature* **358**, 325–327.
- SALA, F. & HERNANDEZ-CRUZ, A. (1990). Calcium diffusion modeling in a spherical neuron. Relevance of buffering system. *Biophysical Journal* **57**, 313–324.
- THELER, J. M., MOLLARD, P., GUÉRINEAU, N., VACHER, P., PRALONG, W. F., SCHLEGEL, W. & WOLLHEIM, C. B. (1992). Video imaging of cytosolic  $\text{Ca}^{2+}$  in pancreatic  $\beta$ -cells stimulated by glucose, carbachol and ATP. *Journal of Biological Chemistry* **267**, 18110–18117.
- THOMAS, P., WONG, J. G., LEE, A. K. & ALMERS, W. (1993). A low affinity  $\text{Ca}^{2+}$  receptor controls the final steps in peptide secretion from pituitary melanotrophs. *Neuron* **11**, 93–104.
- TSE, F. W., TSE, A., HILLE, B., HORSTMANN, H. & ALMERS, W. (1997). Local  $\text{Ca}^{2+}$  release from internal stores controls exocytosis in pituitary gonadotrophs. *Neuron* **18**, 121–132.
- WOLLHEIM, C. B., LANG, J. & REGAZZI, R. (1996). The exocytotic process of insulin secretion and its regulation by  $\text{Ca}^{2+}$  and G-proteins. *Diabetes Review* **4**, 276–297.
- XU, T., NARAGHI, M., KANG, H. & NEHER, E. (1997). Kinetic studies of  $\text{Ca}^{2+}$  binding and  $\text{Ca}^{2+}$  clearance in the cytosol of adrenal chromaffin cells. *Biophysical Journal* **73**, 532–545.

### Acknowledgements

The authors thank E. Pérez and A. Pérez for expert technical assistance. We are also grateful to Dr A. Nadal and Dr F. Sala for helpful comments on the manuscript. The mathematical model was devised by Dr A. Gil and Dr J. Segura. Finally, we are particularly grateful to Dr A. Escobar and Dr J. M. Vergara for their help in the set-up of the spot confocal system. The English was revised by I. Ward. I. Quesada is a recipient of a research studentship from Ministerio de Educación y Cultura. This work was supported in part by grants GV99-139-1-04 (from Generalitat Valenciana), IFD97-1065-CO3-02 (from European Union-CICYT), PM98-0105 and PM99-0142 (from Dirección General de Investigación Científica y Técnica) and 99-1210 (from Fundació Marató TV3).

### Corresponding author

B. Soria: Departamento de Fisiología e Instituto de Bioingeniería, Facultad de Medicina, Campus de San Juan, 03550 San Juan de Alicante, Spain.

Email: bernaat.soria@umh.es